JOURNAL OF SOLID STATE CHEMISTRY 75, 21–29 (1988)

The Magnetic Properties of the Synthetic Langbeinite $KBaCr_2(PO_4)_3$

P. D. BATTLE,* T. C. GIBB, AND S. NIXON

Department of Inorganic and Structural Chemistry, The University, Leeds, LS2 9JT, England

AND W. T. A. HARRISON

Neutron Division, Rutherford Appleton Laboratory, Chilton, Didcot, Oxon., OX11 OQX, England

Received November 2, 1987; in revised form January 6, 1988

The crystal and magnetic structures of the synthetic langbeinite $KBaCr_2(PO_4)_3$ at 1.8 K have been determined from neutron powder diffraction data. The two crystallographically distinct Cr^{3+} sublattices in the cubic structure [space group $P2_13$, $a_0 = 9.7890(1)$ Å] are antiferromagnetically coupled with an ordered magnetic moment of 2.4(2) μ_B per Cr^{3+}. Mössbauer spectroscopy has been used to determine the Néel temperature of an ^{57}Fe-doped sample as 12 K. The effective magnetic moment in the paramagnetic phase has been determined to be 3.84 μ_B per Cr^{3+} ion.

Introduction

Many materials which are isostructural with the mineral langbeinite, $K_2Mg_2(SO_4)_3$, undergo a series of structural phase transitions as a function of temperature and they have been studied extensively for that reason ((*1*, *2*) and references therein). Our own interest in this family of compounds stems from their magnetic properties. Having determined the magnetic structures of $Fe_2(SO_4)_3$ (*3*) and $Fe_2(MoO_4)_3$ (*4*), we attempted to do likewise for the synthetic langbeinite $KBaFe_2(PO_4)_3$ (*5*). Our aim was to compare the strengths of the magnetic superexchange interactions along the different Fe–O–*X*–O–Fe (*X* = Mo, S, or P) pathways found in the three materials, all of which are structurally similar in that they consist of an infinite three-dimensional network made up of FeO_6 octahedra sharing corners with XO_4 tetrahedra. The large interstices in such a structure are empty in $Fe_2(SO_4)_3$ and $Fe_2(MoO_4)_3$ but they are two-thirds occupied by a disordered array of K^+ and Ba^{2+} ions in $KBaFe_2(PO_4)_3$. Although susceptibility and Mössbauer measurements enabled us to show that the latter compound is an antiferromagnet at the lowest temperatures, the Néel temperature of ~4 K is too low to permit a determination of the magnetic structure in a routine neutron diffraction experiment. We have therefore turned our attention to the chromium analog, in the knowledge that $Cr_2(MoO_4)_3$ has a higher Néel temperature (~40 K) than either $Fe_2(SO_4)_3$ (~28 K) or $Fe_2(MoO_4)_3$ (~12 K) (*6*). In this paper we report the first

* To whom correspondence should be addressed.

0022-4596/88 $3.00

determination of the magnetic structure of a langbeinite-like material, $KBaCr_2(PO_4)_3$ (*7*).

Experimental

A polycrystalline sample of $KBaCr_2(PO_4)_3$ was prepared by firing a pelleted stoichiometric mixture of barium carbonate, chromium sesquioxide (both spectroscopic grade), diammonium hydrogen phosphate (Analar), and potassium carbonate at a temperature of 1100°C in a platinum crucible for several weeks, with intermediate grinding and repelleting. Initially, the furnace temperature was raised from 80 to 1100°C at a rate of 300°C per hour, and the final cooling was at a rate of 50°C per hour. The product was a green, poorly sintered pellet (firing at 1200°C did not significantly increase the degree of sintering).

Initial characterization of the compound was by X-ray powder diffraction, and, with the exception of a few very weak lines, the diffraction pattern could be indexed in the cubic space group $P2_13$ with $a_0 = 9.800(1)$ Å, in good agreement with the value of 9.798 Å reported previously by Masse (*7*). The magnetic susceptibility of this sample was measured in the temperature range 80–300 K using a Newport Instruments Gouy balance.

Neutron diffraction data were collected at both room temperature and 1.8 K using the diffractometer D1a at ILL Grenoble, operating at a wavelength of 1.910 Å. The sample was contained in a 12-mm diameter vanadium can which was mounted in a cryostat with an aluminium tail. Each scan over the angular range $0 < 2\theta < 160°$ lasted for ~12 hr using a 2θ step size of 0.05°.

A second sample was prepared with 2% of the Cr replaced by ^{57}Fe, and the Mössbauer spectrum of this sample was recorded at various temperatures between 4.2 and 293 K using a $^{57}Co/Rh$ source matrix held at room temperature; isomer shifts were determined relative to the spectrum of metallic iron.

Results

The temperature dependence of the inverse magnetic susceptibility (Fig. 1) indi-

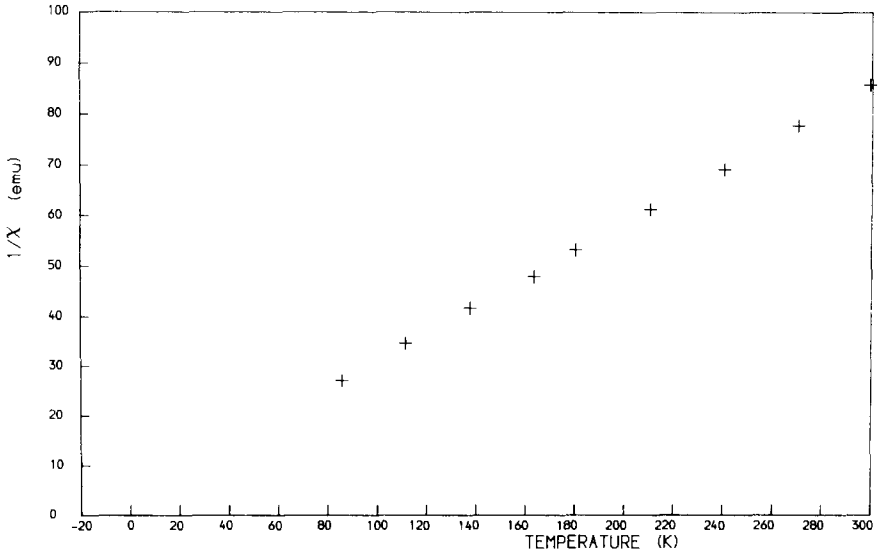

FIG. 1. The temperature dependence of the inverse molar magnetic susceptibility of $KBaCr_2(PO_4)_3$.

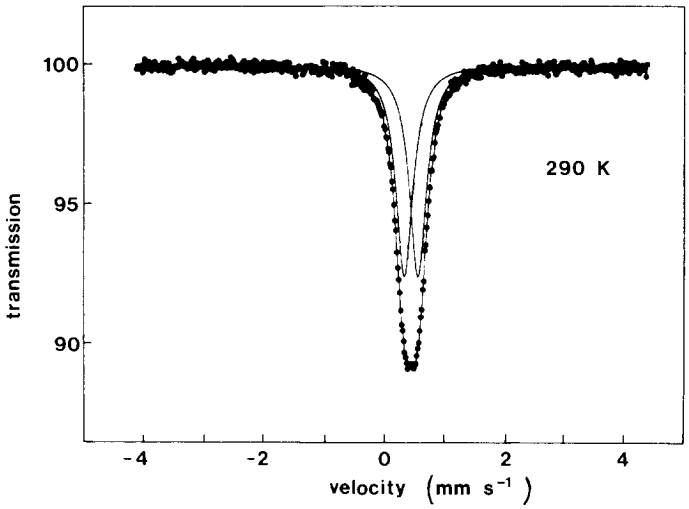

FIG. 2. The observed and calculated Mössbauer spectra of $^{57}Fe/KBaCr_2(PO_4)_3$ at 290 K.

cates that $KBaCr_2(PO_4)_3$ is paramagnetic throughout the measured range. The value of the effective magnetic moment per Cr^{3+} deduced from our data (3.84 μ_B) is in good agreement with the spin-only value (3.87 μ_B), as would be expected for a $3d^3:{}^4A_{2g}$ ion in octahedral coordination.

The Mössbauer data collected at room temperature are plotted in Fig. 2 and show a comparatively sharp resonance with a very small splitting. The langbeinite structure is known to consist of two chemically similar, but crystallographically distinct, distorted octahedral sites for the transition metal (5). We have chosen to interpret the observed spectrum as one quadrupole-split doublet, thus assuming that the similarity between the two sites is such that any differences in their spectra are too small to be resolved. We prefer this model to an interpretation involving the two unsplit singlets, one corresponding to each site, because the isomer shift is generally not sensitive to only small changes in the chemical environment. The refined values of the isomer shift (δ), quadrupole splitting (Δ), and Lorentzian linewidth (Γ) for this paramagnetic phase are presented in Table I. Variable temperature Mössbauer spectroscopy enabled us to determine the Néel temperture of $KBaCr_2(PO_4)_3$ as 12.0 ± 0.5 K. Below this temperature the observed spectrum broadened into a pattern showing six-line magnetic hyperfine splitting; the data recorded at 6.5 and 4.2 K are shown in Fig. 3. The linewidths are extremely broad, but we were unable to resolve the hyperfine fields from the two different crystallographic sites at any temperature between 4.2 and 12 K. The observed absorption lines show no sign of substructure, and we conclude that this indicates the existence of a broad distribution in the values of the hyperfine field. The disordered arrangement of the K^+ and Ba^{2+} ions in the structure, the relatively weak magnetic coupling experienced by the ^{57}Fe dopant in the Cr^{3+} sublattice, and the

TABLE I

MÖSSBAUER PARAMETERS FOR PARAMAGNETIC $^{57}Fe/KBaCr_2(PO_4)_3$ AT 290 K

δ (mm sec^{-1})	Δ (mm sec^{-1})	Γ (mm sec^{-1})
0.454(2)	0.226(2)	0.343(3)

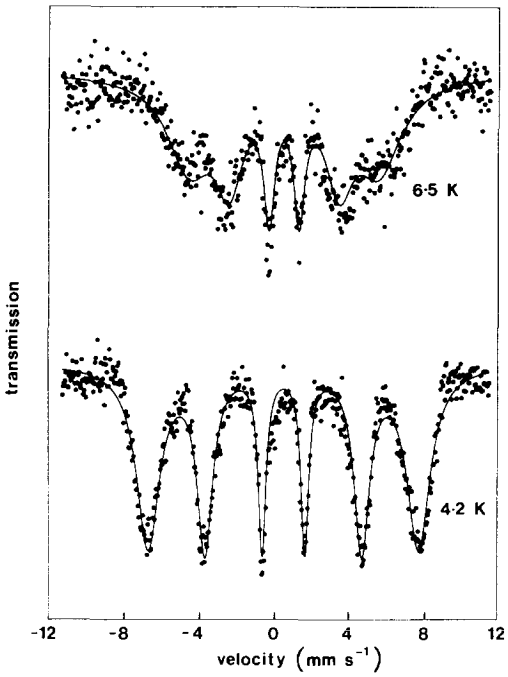

FIG. 3. The observed and calculated Mössbauer spectra of $^{57}Fe/KBaCr_2(PO_4)_3$ at 4.2 and 6.5 K.

presence of two crystallographic sites will all contribute to this effect. The exact distribution of hyperfine field values remains unknown, and we have attempted to simulate the effect using a simple model with only one field value, but with the linewidth of the nth line, Γ_n, described by the function $\Gamma_n = \Gamma_0(1 + p_n\Gamma_{\text{eff}})$ where p_n is the fractional displacement from the centroid of the sextet of the nth line along the baseline (thus $p_n = 0.1578$ for $n = 3$ or 4, $= 0.5789$ for $n = 2$ or 5, $= 1$ for $n = 1$ or 6). The quadrupole splitting was set to zero and the relative line intensities were constrained to be in the ratios 3 : 2 : 1 : 1 : 2 : 3 as expected for a randomly orientated polycrystalline sample of negligible thickness. This simple model gave a reasonable simulation of the data at 4.2 K. The data collected at 6.5 K were treated in a similar manner except that Γ_0 was held constant at the value determined from the 4.2 K data. The refined parameters are listed in Table II, and the corresponding calculated curves are shown in Fig. 3. There was no significant improvement in the agreement between the observed and calculated spectra when two hyperfine fields were included in the refinements.

The neutron diffraction data collected at room temperature were analyzed by the Rietveld profile analysis technique (*8*) in the space group $P2_13$ taking the structure of $KBaFe_2(PO_4)_3$ (*5*) as a starting model. It became clear that our sample was contaminated with a second phase, identified as Cr_2O_3, and we therefore used a multipattern profile analysis program (*9*) in order to refine simultaneously the structural parameters of $KBaCr_2(PO_4)_3$ and Cr_2O_3. Those regions of the profile which showed either an asymmetric peak shape ($2\theta < 30°$) or scattering from the cryostat were excluded from the refinements, which converged to give $R_{\text{wpr}} = 8.8\%$. The data collected at 1.8 K showed some marked differences, particularly at low 2θ values, from those taken at room temperature, but these differences were all accounted for by the model for the magnetic structure to be discussed below. In particular, there was considerable enhancement of the intensities of the {110}, {200}, and {120} Bragg peaks. This led us to conclude that the crystallographically distinct chromium ions were coupled together antiferromagnetically and the subsequent data analysis has confirmed this. The four symmetry-related Cr(1) ions form one ferromagnetic sublattice and the four Cr(2)

TABLE II

MÖSSBAUER PARAMETERS FOR ANTIFERROMAGNETIC $^{57}Fe/KBaCr_2(PO_4)_3$

T (K)	δ (mm sec^{-1})	Γ_0 (mm sec^{-1})	Γ_{eff} (mm sec^{-1})	B (T)
6.5	0.56(2)	0.31	8.2(3)	31.53(4)
4.2	0.57(1)	0.31(2)	3.8(3)	44.98(1)

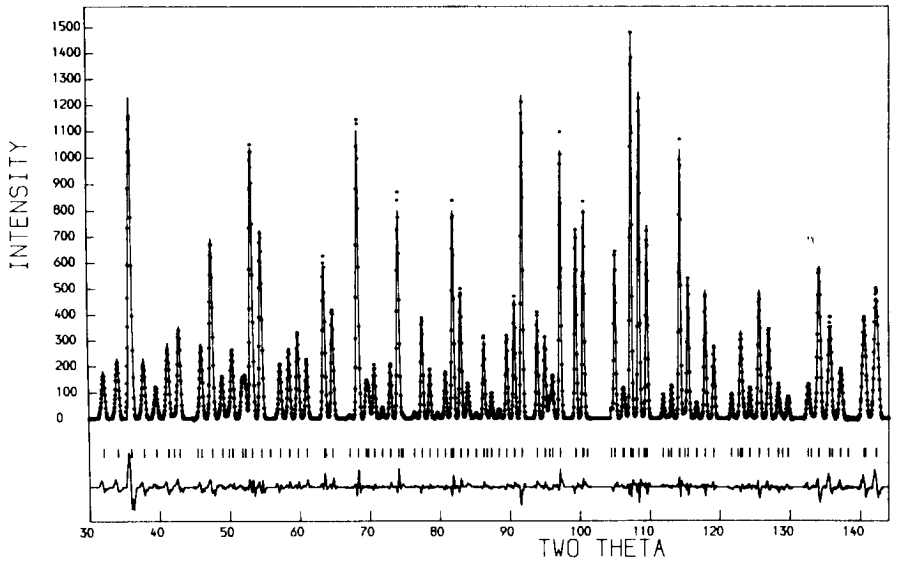

FIG. 4. The observed, calculated, and difference diffraction profiles at 1.8 K of $KBaCr_2(PO_4)_3$ contaminated by Cr_2O_3. Reflection positions are marked.

ions form another, the two sublattices having equal and opposite magnetizations. The diffraction data were analyzed by multipattern profile analysis, the data with $2\theta < 30°$ again being omitted because of asymmetric peak profiles. The strongest magnetic peaks of Cr_2O_3 were excluded from the refinements and the free-ion form factor (*10*) was used to describe the angular variation of the magnetic scattering length of Cr^{3+} in KBa $Cr_2(PO_4)_3$. Least-squares analysis of 19 atomic coordinates, an occupation number, an overall temperature factor, the magnetic moment and the profile parameters for the langbeinite, plus two atomic coordinates and the profile parameters for Cr_2O_3, resulted in a final $R_{wpr} = 8.0\%$. The occupation number was refined in order to allow a partially ordered arrangement of K^+ and Ba^{2+} over the two appropriate sites in the structure. The final observed and calculated diffraction patterns are shown in Fig. 4; the reflection positions marked in the figure are those of both $KBaCr_2(PO_4)_3$ and Cr_2O_3. The refined atomic coordinates are given in Tables III and IV; they do not differ significantly from those found at room temperature and the latter are therefore not tabulated separately. The most important bond lengths and bond angles in $KBaCr_2(PO_4)_3$ are listed in Table V. The ordered

TABLE III

STRUCTURAL PARAMETERS FOR $KBaCr_2(PO_4)_3$ AT 1.8 K

Atom type	Site	x	y	z
K/Ba(1)[a]	4a	0.0677(4)	0.0677(4)	0.0677(4)
K/Ba(2)[b]	4a	0.2960(5)	0.2960(5)	0.2960(5)
Cr(1)	4a	0.5875(5)	0.5875(5)	0.5875(5)
Cr(2)	4a	0.8527(5)	0.8527(5)	0.8527(5)
P	12b	0.6258(3)	0.4594(3)	0.2739(5)
O(1)	12b	0.6528(3)	0.4950(3)	0.4237(4)
O(2)	12b	0.7616(3)	0.4854(3)	0.1975(3)
O(3)	12b	0.5784(4)	0.3117(3)	0.2594(3)
O(4)	12b	0.5214(3)	0.5513(3)	0.2028(3)

Note. Space group $P2_13$; $a_0 = 9.7890(1)$ Å; $B_{overall} = 0.41(2)$ Å^2.

[a] 82% Ba, 18% K (±4% e.s.d.).

[b] 18% Ba, 82% K.

TABLE IV

STRUCTURAL PARAMETERS FOR Cr_2O_3 AT 1.8 K

Atom type	Site	x	y	z
Cr	12c	0	0	0.3498(5)
O	18e	0.3067(9)	0	$\frac{1}{4}$

Note. Space group $R\bar{3}c$; a_0 = 4.9516(4), c_0 = 13.5987(6) Å.

component of the magnetic moment refined to a value of 2.4(2) μ_B per Cr^{3+} ion; no information regarding the direction of the moment can be deduced from an experiment which utilizes a polycrystalline sample of a cubic material.

Discussion

The results described above all indicate that $KBaCr_2(PO_4)_3$ is isostructural with the mineral langbeinite, $K_2Mg_2(SO_4)_3$, that it is paramagnetic above 12 K, and antiferromagnetic below that temperature. The bond lengths and bond angles found for the trigonally distorted CrO_6 octahedra are all chemically resonable and the extent of the distortion of the PO_4 tetrahedron is similar to that found in $KBaFe_2(PO_4)_3$. The most obvious structural difference between the Fe^{3+} and Cr^{3+} compounds is that the potassium and barium ions are disordered over the nine-coordinate 4a sites in the former, whereas there is a significant partial ordering in $KBaCr_2(PO_4)_3$. This is reasonable in view of the markedly different coordination geometries around the two sites in the Cr compound (Figs. 5 and 6); K/Ba(1) lies asymmetrically between a puckered six-membered ring of oxygen atoms and a further three oxygens, whereas K/Ba(2) lies close to the center of a tricapped antiprism.

It is obviously undesirable to work with an impure sample, but the use of the multipattern Rietveld program has enabled us to do so in a satisfactory way; the structural parameters give in Table IV for Cr_2O_3 are in good agreement with the published values (*11*). The impurity was not detected at an earlier stage because it is a very weak X-ray scatterer, and the solubility of our product

TABLE V

BOND LENGTHS (IN Å) AND BOND ANGLES (IN DEGREES) FOR $KBaCr_2(PO_4)_3$ AT 1.8 K

K/Ba(1)–O(1)	2.829(9)	(×3)	K/Ba(2)–O(2)	3.093(9)	(×3)
K/Ba(1)–O(2)	2.954(9)	(×3)	K/Ba(2)–O(3)	2.792(9)	(×3)
K/Ba(1)–O(4)	2.927(9)	(×3)	K/Ba(2)–O(4)	2.989(9)	(×3)
Cr(1)–O(1)	1.95(1)	(×3)	P–O(1)	1.530(9)	
Cr(1)–O(2)	1.96(1)	(×3)	P–O(2)	1.547(9)	
Cr(2)–O(3)	1.97(1)	(×3)	P–O(3)	1.525(9)	
Cr(2)–O(4)	1.98(1)	(×3)	P–O(4)	1.529(9)	
O(1)–Cr(1)–O(1)	92.3		O(2)–P–O(1)	106.1	
O(2)–Cr(1)–O(1)	92.0		O(3)–P–O(1)	111.0	
O(2)–Cr(1)–O(1)	82.6		O(4)–P–O(1)	114.8	
O(2)–Cr(1)–O(1)	173.4		O(3)–P–O(2)	111.8	
O(2)–Cr(1)–O(2)	93.4		O(4)–P–O(2)	104.9	
O(3)–Cr(2)–O(3)	93.4		O(4)–P–O(3)	108.2	
O(4)–Cr(2)–O(3)	88.6				
O(4)–Cr(2)–O(3)	175.9				
O(4)–Cr(2)–O(3)	90.0				
O(4)–Cr(2)–O(4)	87.9				

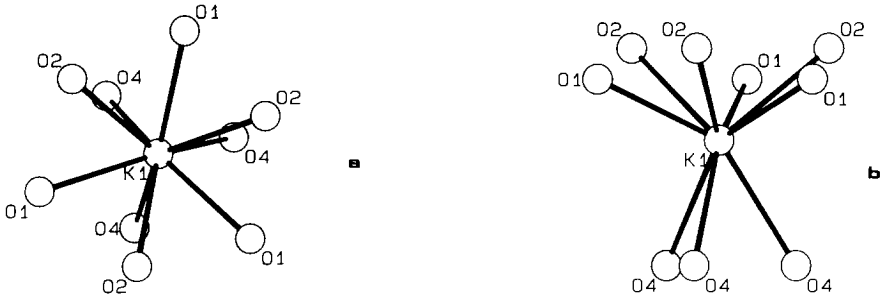

FIG. 5. The environment of the site K/Ba(1), viewed (a) down ⟨111⟩ and (b) perpendicular to ⟨111⟩.

was so low as to preclude the use of traditional analysis methods. The good agreement between the observed effective magnetic moment in the paramagnetic region and the spin-only value suggests that the impurity concentration is low, and the absence of any hyperfine splitting in the room-temperature Mössbauer pattern indicates that our ^{57}Fe-doped sample was free of Cr_2O_3, for which T_N = 318 K (*12*).

The low-temperature magnetic structure of $KBaCr_2(PO_4)_3$ is that which would have been predicted in the light of earlier results in $Fe_2(SO_4)_3$ and $Fe_2(MoO_4)_3$. Each Cr^{3+} ion is magnetically coupled to other Cr^{3+} ions by a total of 18 superexchange pathways: 6 of these pathways lead to an ion that is crystallographically equivalent to the central Cr^{3+} whereas the other 12 pathways lead to a crystallographically distinct ion; for example, a Cr(1) ion has six magnetic links with other Cr(1) ions, but 12 with Cr(2) ions (see Fig. 7). The observed magnetic structure having the Cr(1) and Cr(2) sublattices coupled antiferromagnetically, thus stabilizes the inherent antiferromagnetic coupling between pairs of d^3 ions to the greatest possible extent. The ordered magnetic moment of 2.4(2) μ_B per Cr^{3+} ion is comparable to that of 2.5(2) μ_B deduced previously (*6*) for $Cr_2(MoO_4)_3$, but it should be remembered that the value obtained is dependent on the form factor assumed in the analysis of the diffraction data. However, the departure of the true form factor from the free-ion curve used in our calculations is unlikely to be large enough to take the value beyond the statistical error limits quoted.

The room-temperature Mössbauer parameters reported in Table I for ^{57}Fe/KBa $Cr_2(PO_4)_3$ are characteristic of high-spin

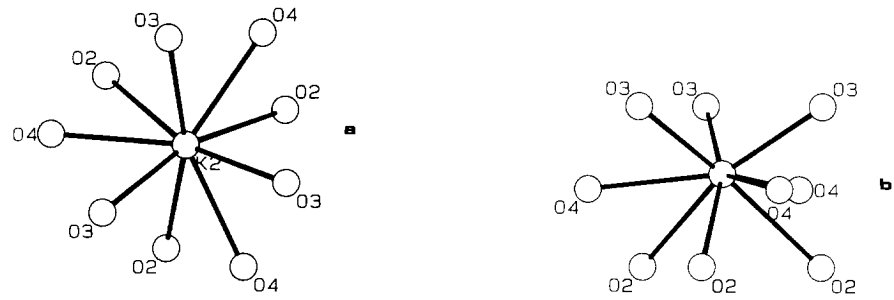

FIG. 6. The environment of the site K/Ba(2), viewed (a) down ⟨111⟩ and (b) perpendicular to ⟨111⟩.

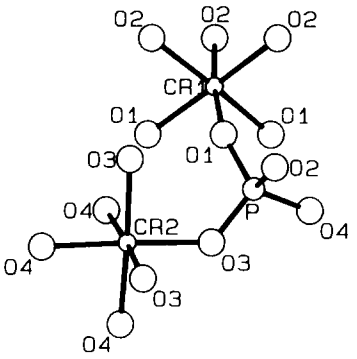

FIG. 7. A fragment of the structure of $KBaCr_2(PO_4)_3$, showing the superexchange pathway between sites Cr(1) and Cr(2).

Fe^{3+} in an octahedral site and need no further comment. The spectra recorded at 4.2 and 6.5 K are more interesting. We have already referred to the broadening of the spectral lines observed below the Néel temperature, and this phenomenon, indicating the presence of a range of hyperfine fields at ^{57}Fe sites, can be attributed, in part, to the partial disorder of the K^+ and Ba^{2+} ions and also to the presence of two distinct Fe^{3+} sites. However, it may also represent a relatively weak coupling of the dopant cation to the magnetic structure. The flux density, B, of the hyperfine field of ~45 T observed at 4.2 K is rather low for Fe^{3+} in a compound well below the Néel temperature and, furthermore, the decrease in field observed between 4.2 and 6.5 K is greater than would be expected in Brillouin-like behavior. Although it was possible to analyze the Mössbauer data of $KBaFe_2(PO_4)_3$ in terms of two hyperfine fields (*5*), it is clearly inappropriate to use the same approach in dealing with the ^{57}Fe-doped chromium analog. The weak coupling between host and dopant may be due to a ferromagnetic component in the superexchange between Fe^{3+} and Cr^{3+} which is absent in interactions between like ions of either type.

It is pleasing to find that our decision to use a chromium compound to determine the magnetic structure of a langbeinite was justified, in that the Néel temperature is 12 K, compared to the value of 4 K found previously for the iron analog (*5*). This demonstrates once again (*6*) the great strength of the π-superexchange in these materials, the e_g orbitals being unoccupied for $Cr^{3+}: 3d^3$ and the rapid increase in the strength of the superexchange as the length of the pathway decreases. Indeed the ratio of the Néel temperatures of the iron and chromium langbeinites is very similar to that between the iron and chromium molybdates (T_N = 12 and 40 K, respectively); the reasons for the lowering of the Néel temperature in the case of the phosphates have been discussed previously (*5*). The presence of two crystallographically distinct transition metal sites in this structure gives rise to the possibility of L-type ferrimagnetism (*13*), that is the incomplete cancellation of the magnetizations of the two sublattices at temperatures between absolute zero and T_N (or more properly, T_C). This effect has been seen clearly in $Fe_2(SO_4)_3$ and $Fe_2(MoO_4)_3$, but was apparently absent in $Cr_2(MoO_4)_3$; there was some evidence for it in $KBaFe_2(PO_4)_3$. The experimental techniques available to us have been unable to identify any imbalance in the sublattice magnetizations in $KBaCr_2(PO_4)_3$, although low temperature magnetization measurements might clarify this point.

Acknowledgments

We are grateful to the SERC for financial support and to Dr. A. W. Hewat for assistance at ILL Grenoble.

References

1. N. YAMADA, N. MAEDA, AND H. ADACHI, *J. Phys. Soc. Japan.* **50,** 907 (1981).
2. D. SURESH BABU, G. S. SASTRY, M. D. SASTRY, AND A. G. I. DALVI, *J. Phys. C* **17,** 4245 (1984).

3. G. J. LONG, G. LONGWORTH, P. D. BATTLE, A. K. CHEETHAM, R. V. THUNDATHIL, AND D. BEVERIDGE, *Inorg. Chem.* **18,** 624 (1979).
4. P. D. BATTLE, A. K. CHEETHAM, G. J. LONG, AND G. LONGWORTH, *Inorg. Chem.* **21,** 4223 (1982).
5. P. D. BATTLE, A. K. CHEETHAM, W. T. A. HARRISON, AND G. J. LONG, *J. Solid State Chem.* **62,** 16 (1986).
6. P. D. BATTLE, A. K. CHEETHAM, W. T. A. HARRISON, N. J. POLLARD, AND J. FABER, *J. Solid State Chem.* **58,** 221 (1985).
7. R. MASSE, *Bull. Soc. Fr. Mineral. Cristallogr.* **95,** 405 (1972).
8. H. M. RIETVELD, *J. Appl. Crystallogr.* **2,** 65 (1969).
9. M. W. THOMAS AND P. J. BENDALL, *Acta Crystallogr. Sect. A* **34**(s), S351 (1978).
10. R. E. WATSON AND A. J. FREEMAN, *Acta Crystallogr.* **14,** 27 (1961).
11. R. W. G. WYCKOFF, "Crystal Structures," Vol. 2, Wiley–Interscience, New York (1964).
12. B. N. BROCKHOUSE, *J. Chem. Phys.* **21,** 961 (1953).
13. L. NÉEL, *Ann. Phys.* **3**(12), 137 (1948).